

Dissolution and gettering of iron during contact co-firing

J-F. Lelièvre^{a*}, J. Hofstetter^b, A. Peral^b, I. Hoces^c, F. Recart^c and C. del Cañizo^b

^a *Centro de Tecnología del Silicio Solar, Eric Kandel 1, TecnoGetafe, 28905 Getafe, Madrid, Spain*

^b *Instituto de Energía Solar, Universidad Politécnica de Madrid, Ciudad Universitaria, 28040 Madrid, Spain*

^c *TiM, Instituto de Tecnología Microelectrónica Parque Tecnológico de Bizkaia, 48170 Zamudio, Bilbao, Spain*

Abstract

The dissolution and gettering of iron is studied during the final fabrication step of multicrystalline silicon solar cells, the co-firing step, through simulations and experiments. The post-processed interstitial iron concentration is simulated according to the as-grown concentration and distribution of iron within a silicon wafer, both in the presence and absence of the phosphorus emitter, and applying different time-temperature profiles for the firing step. The competing effects of dissolution and gettering during the short annealing process are found to be strongly dependant on the as-grown material quality. Furthermore, increasing the temperature of the firing process leads to a higher dissolution of iron, hardly compensated by the higher diffusivity of impurities. A new defect engineering tool is introduced, the extended co-firing, which could allow an enhanced gettering effect within a small additional time.

Keywords: multicrystalline silicon, co-firing step, Rapid Thermal Annealing, iron, extended gettering, defect engineering

1. Introduction

During the last years, the rapid growth of the photovoltaic (PV) industry has changed the polysilicon market completely, focusing the attention to the so-called solar grade silicon (SoG-Si), whose impurity requirements are less restrictive than those of electronic grade silicon (eg-Si) [1, 2]. The need of reducing the production costs while maintaining the solar cell efficiency high demands the investigation of defect engineering tools to reduce or neutralize impurities during the solar cell fabrication process [3, 4]. It is necessary to consider the whole thermal history of the solar silicon material, from the SoG-Si to the solar cell, in order to take into account the effect of high temperature steps on the metal impurity concentrations

* Corresponding author. Tel.: +34 91 126 00 37; fax: +34 91 544 63 41.

E-mail address: jf.lelievre@centesil.es.

within the Si material. The first high temperature step is the crystallization process. For instance, directional solidification of multicrystalline silicon (mc-Si) ingots allows a 2 to 3 order of magnitude reduction of metal impurity contamination through solid-liquid segregation [2]. After crystallization, it is admitted that interstitial iron (Fe_i) is usually the dominant lifetime-limiting defect in most mc-Si wafers. In a typical industrial mc-Si solar cell fabrication chain, the next high temperature step is the Phosphorus Diffusion Gettering (PDG) at about 800-900°C for several minutes. It has been extensively investigated, showing that it leads to a good reduction of the interstitial iron concentration $[\text{Fe}_i]$ for standard mc-Si material. For SoG-Si, efforts have been focused on the development of defect engineering tools, such as extended gettering, for further metal impurity concentration reduction [3, 4]. It has been highlighted that the gettering efficiency depends strongly on the as-grown Fe concentration and distribution (Fe precipitate density and radius) [3, 5]. However, very little attention has been paid to the last high temperature step included at the end of the solar cell fabrication process: the co-firing step.

The co-firing step is usually carried out in an infrared lamps belt furnace to form the screen-printed front and back metallic contacts. During this short step at about 800-900°C, atomic hydrogen contained in the silicon nitride (SiN) anti-reflection coating diffuses and passivates defects deep into the bulk of the Si substrate [6, 7]. There has been an ongoing discussion if only crystalline defects (e.g. dislocations) or also metallic impurities are passivated by hydrogen, as some authors [8, 9] measured a reduction of $[\text{Fe}_i]$ after SiN Rapid Thermal Annealing (RTA). However, Bentzen et al. [10] found that only grains of low metal content are effectively H-passivated. Moreover, Tan et al. [6] demonstrated that the improvement in lifetime is primarily caused by the passivation of other recombination active defects apart from Fe_i . On the contrary, the firing step is likely to produce the partial dissolution of Fe precipitates, which could partly offset the $[\text{Fe}_i]$ reduction obtained during PDG [6, 11]. Furthermore, it has been claimed [12] that the phosphorous emitter can act as “protective layer” during RTA, minimizing the increase of $[\text{Fe}_i]$. However, no clear explanation has been given to date to interpret the different results obtained.

With the help of our recently developed Impurity-to-Efficiency (I2E) simulation tool [5], this paper examines the dissolution and gettering of iron during the co-firing step. As it is a complex process, due to multiple parameters interactions (ohmic front and back contact formation, Back Surface Field creation, hydrogenation from the SiN layer, P and Al gettering effects, screen-printing pastes compatibility...), in a first step, we have focused the study on the P gettering effect during RTA. The final $[\text{Fe}_i]$ has been determined through simulations as a function of the as-grown Fe concentration and distribution within a mc-Si wafer, both in the presence and absence of the P emitter. At the same time, experiments were performed to test the predicted trends, confirming that both precipitate dissolution and external gettering of iron to the P diffused layer take place during the RTA process. The possibility to develop new defect engineering tools with the help of I2E simulations has also been tested and confirmed.

2. Experimental details

In a first experiment dedicated to the study of dissolution of Fe precipitates during the RTA step, 4.5×4.5 cm² mc-Si wafers from the same ingot were subjected to a standard chemical cleaning, before P diffusion at 850°C during 20 min in a quartz tube furnace. These wafers were then chemically etched to remove the P emitter and SiN was deposited on both sides for surface passivation. After measuring $[\text{Fe}_i]$ through Fe-B pair dissociation [13], the mc-Si wafers were annealed in an industrial belt furnace with different RTA time-temperature profiles, and $[\text{Fe}_i]$ was measured again.

In a second experiment dedicated to the study of the P gettering effect during RTA, 28 mc-Si sister wafers (4.5×4.5 cm²) were taken from the middle of the central brick of an industrial mc-Si ingot. After chemical cleaning and P diffusion (850°C – 20min), the wafers were dipped into HF to remove the P₂O₅ glass. Then, they were subjected to a RTA process in a laboratory furnace. In different RTA processes,

the peak time and temperature (t_{peak} and T_{peak} , respectively) as well as the cool down rate $\Delta T/t$ were modified. Subsequently, the wafers were chemically etched to remove the P emitter before the PECVD deposition of SiN on both sides. Finally, effective lifetime and $[\text{Fe}_i]$ were measured using the QSS-PC technique ($\Delta n = 10^{15} \text{ cm}^{-3}$). Some of the as-grown and P-diffused wafers had been set aside as control wafers. In order to investigate wafers with a higher Fe concentration, another 10 sister wafers were taken from 85% ingot height of a corner brick and were processed in the same way as described herein.

3. Results

3.1. Dissolution of iron during co-firing

Experimental and simulation results show that a short annealing in the absence of the P emitter leads to dissolution of iron precipitates (presumably $\beta\text{-FeSi}_2$), and consequently to an increase of $[\text{Fe}_i]$. Figure 1.a shows the experimental Fe_i concentration after PDG (black stars) and after RTA, using different t_{peak} and T_{peak} . A rather homogeneous post-processed $[\text{Fe}_i]$ is found after PDG, with values lying between 1 and $3 \times 10^{11} \text{ cm}^{-3}$. For all mc-Si wafers, $[\text{Fe}_i]$ increases drastically after RTA in the absence of the P emitter, with final values generally well above the as-grown ones. However, these experimental results do not indicate a clear trend of the post-processed $[\text{Fe}_i]$, neither as a function of the time-temperature profile, nor of the as-grown $[\text{Fe}_i]$. Simulations indicate that the as-grown iron concentration and distribution have a strong impact on the post-processed $[\text{Fe}_i]$ (see Fig 1.b). They show that an equal as-grown Fe concentration approximately leads to an equal post-processed $[\text{Fe}_i]$ independently of the as-grown $[\text{Fe}_i]$. On the contrary, the same as-grown $[\text{Fe}_i]$ associated to different as-grown Fe concentrations (and distributions) leads to significantly different post-processed $[\text{Fe}_i]$. This indicates that a large dispersion of the post-processed concentrations can be obtained within the same mc-Si ingot (see Fig 1.a). Nevertheless, experiments confirm that precipitates dissolution takes place during the short co-firing step. Furthermore, for one particular as-grown iron concentration and distribution, simulations show that increasing t_{peak} leads to a higher post-processed $[\text{Fe}_i]$ (not shown here). An even more detrimental $[\text{Fe}_i]$ increase is obtained when increasing T_{peak} (see Fig 2.a). However, it can be noted that all post-processed $[\text{Fe}_i]$ values stay well below the solid solubility of the respective peak temperature, as the process time is

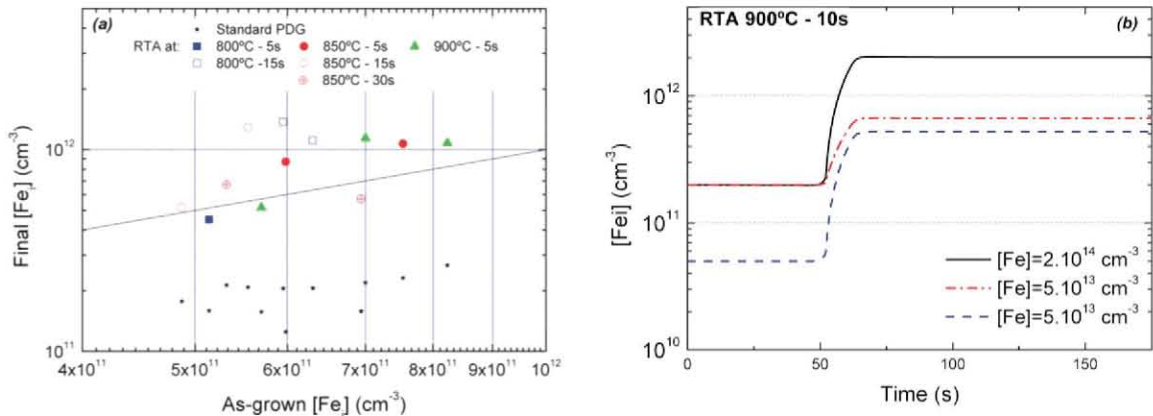


Fig. 1. (a) Post-processed $[\text{Fe}_i]$ of gettered mc-Si wafers as a function of as-grown $[\text{Fe}_i]$ for different time-temperature profiles; no P emitter is present. The line indicates the limit for which $[\text{Fe}_i]_{\text{Final}} = [\text{Fe}_i]_{\text{as-grown}}$ (b) Simulated $[\text{Fe}_i]$ as a function of time during a 10s RTA at 900°C for different as-grown Fe concentrations and precipitate densities (precipitate radius $r_0 = 30 \text{ nm}$) and different as-grown $[\text{Fe}_i]$ (values at $t=0$).

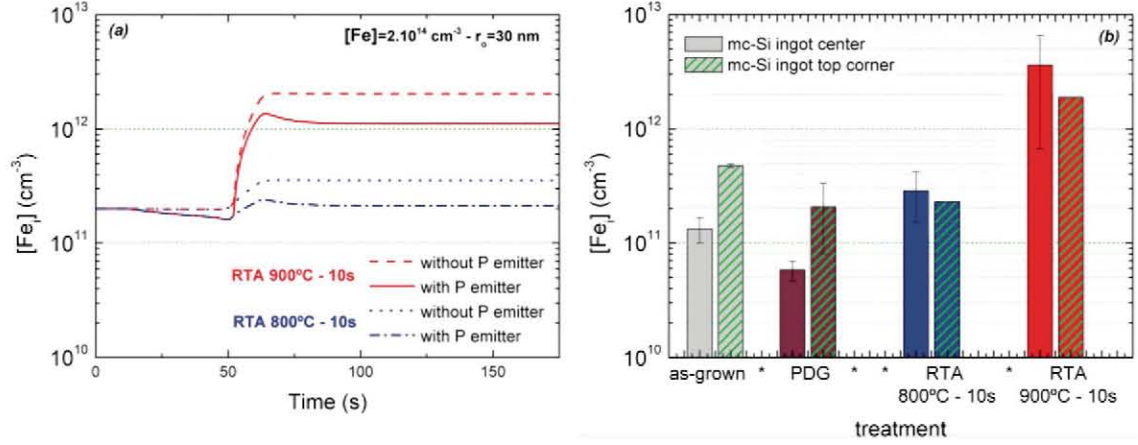


Fig. 2. (a) Simulated $[Fe_i]$ as a function of time during a 10s RTA at 800°C and 900°C, with and without P emitter, respectively, for an arbitrary as-grown Fe concentration and distribution ($[Fe_i]_{as-grown} \approx 2 \cdot 10^{11} cm^{-3}$). (b) As-grown and post-processed experimental $[Fe_i]$ of mc-Si wafers taken from the center and top-corner of an industrial ingot.

very short. These observations lead to the conclusion that t_{peak} and T_{peak} should be minimized in order to reduce the precipitates dissolution effect during contact firing.

3.2. Gettering of iron during co-firing

Simulations indicate that a slight external gettering effect occurs during the short firing step when the P emitter is present (see Fig 2a). Thus, the dissolution of precipitates is partly compensated during the high temperature process and the subsequent cooling to room temperature. However, increasing T_{peak} leads to a higher dissolution of iron which is hardly compensated by its higher diffusivity.

Figure 2.b shows the experimental results obtained for mc-Si wafers taken from the center and from the top-corner of the mc-Si ingot. As-grown $[Fe_i]$ are significantly different, indicating different cooling down profiles during crystallization. Furthermore, mc-Si wafers from the top of the ingot are expected to exhibit a higher total Fe concentration accompanied with higher precipitate density and radius [14]. After PDG, center wafers show a drastic reduction of $[Fe_i]$ to values well below $10^{11} cm^{-3}$, whereas for top-corner mc-Si wafers, the $[Fe_i]$ reduction is rather small. After the RTA process, $[Fe_i]$ increases for central wafers, indicating precipitate dissolution. Furthermore, a higher T_{peak} leads to a higher $[Fe_i]$. On the other hand, for mc-Si wafers taken from the top-corner of the ingot, no increase of the interstitial iron concentration is observed for a standard process at 800°C. As experiments without P emitter showed precipitate dissolution in all cases, we can conclude on a slight gettering effect during co-firing when the P emitter is present. However, the results highlight the need to carefully select the appropriate time-temperature profile for PDG and RTA processes when using Si wafers of different material qualities. This is especially important for the RTA temperature profile when low $[Fe_i]$ is obtained after PDG.

3.3. Extended gettering of iron during co-firing

We used our I2E simulation tool to find a short optimized RTA temperature profile in order to minimize the detrimental effect of precipitate dissolution. For this purpose, we optimized the cool down profile under the constraint of keeping the co-firing step short (extra time $< 2''$). In the following, we will refer to the optimized process as “extended co-firing” (or “extended RTA”). In comparison with standard

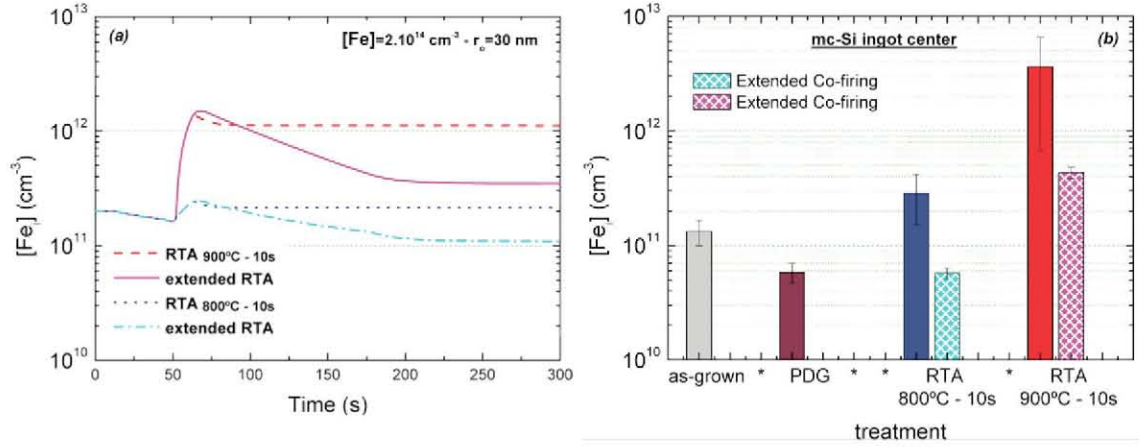


Fig. 3. (a) Simulated $[Fe_i]$ as a function of time during a 10s standard and extended RTA, for an arbitrary as-grown Fe concentration and distribution. (b) Measured $[Fe_i]$ obtained for mc-Si wafers taken from the center of an industrial ingot.

RTA, the extended RTA is expected to lead to an enhanced segregation gettering effect to the P emitter (see Fig. 3.a). Experimental results confirm this trends, showing only a moderate increase of $[Fe_i]$ for $T_{peak}=900^\circ C$ in comparison to the standard RTA process (see Fig 3.b). Furthermore, for $T_{peak}=800^\circ C$, we obtained a complete compensation of precipitates dissolution, which indicates the high potential of such a short process for its industrial application. However, QSS-PC measurements show that lifetime is not fully recovered by the extended co-firing step (see Fig 4). This could be explained by the contamination through other metal impurities as well as crystal degradation during the high temperature process. However, it is highly possible that lifetime will be further improved by SiN hydrogenation and Al gettering, and further studies are needed to evaluate separately each parameter.

For wafers from the ingot top-corner (not shown here), an extended gettering effect is observed but the $[Fe_i]$ reduction is lower than for wafers from ingot center. In this case, it seems that extended co-firing has to be further optimized. However, a further increase of the RTA process time is impeded by other process parameters such as hydrogenation and screen-printing paste compatibility. Thus, in order to maximize the gettering efficiency and effectively reduce $[Fe_i]$, it is necessary to optimize the time-temperature profile of the whole solar cell fabrication process, including the PDG.

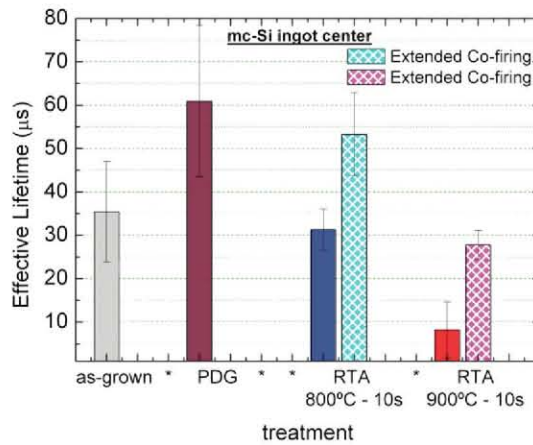


Fig. 4. As-grown and post-processed effective lifetime obtained for mc-Si wafers taken from the center of an industrial ingot.

4. Conclusion

We have shown through simulations and experiments that Fe precipitate dissolution and Fe_i external gettering occur during the short co-firing step, strongly depending on the as-grown Fe concentration and distribution. During standard co-firing, a slight gettering effect can partly compensate precipitate dissolution. However, a much better $[\text{Fe}_i]$ reduction is obtained through the extended co-firing process that we introduced. Therefore, it is shown that the I2E simulation tool can guide towards optimum process conditions according to the material properties and the solar cell architecture, and it can be used for the design of new defect engineering tools.

Acknowledgements

This work has been partially funded by the Spanish Ministerio de Ciencia e Innovación, through the project Thincells (TEC2008-06798-C03-02). The authors want to thank DC Wafers for wafer supply.

References

- [1] Crystal Clear Workshop “Arriving at well-founded specifications for SoG Si feedstock”, Amsterdam, The Netherlands, 13th-14th November 2008.
- [2] J. Hofstetter, J.F. Lelièvre, C. del Cañizo, A. Luque. Acceptable contamination levels in solar grade silicon: from feedstock to solar cell. *Material Science & Engineering B* 2009; **159-160**: 299-304.
- [3] T. Buonassisi, et al. Engineering metal-impurity nanodefects for low-cost solar cells. *Nature Materials* 2005; **4**:676-679.
- [4] M. Rinio, et al. Improvement of multicrystalline silicon solar cells by a low temperature anneal after emitter diffusion. *Progress in Photovoltaics: Research and Applications* 2011; **19-2**: 165-169.
- [5] J. Hofstetter, et al. Impurity-to-Efficiency Simulator: Predictive Simulation of Solar Cell Efficiency Based on Iron Content and Distribution. *Progress in Photovoltaics: Research and Applications* 2011; **19-3**: in press, DOI: 10.1002/pip.1062
- [6] J. Tan, et al. Optimised gettering and hydrogenation of multi-crystalline silicon wafers for use in solar cells. *Proceedings of the 22nd EUPVSEC*, Milan, Italy, 2007, pp. 1309–1313.
- [7] J-F. Lelièvre, et al. Study of the composition of hydrogenated silicon nitride SiN_xH for efficient surface and bulk passivation of silicon. *Solar Energy Materials and Solar Cells* 2009; **93-8**: 1281-1289.
- [8] A. Azzizi, L.J. Geerligs and D. Macdonald. Hydrogen passivation of iron in crystalline silicon. *Proceedings of the 19th EUPVSEC*, Paris, France, 2004, pp. 1021-1024.
- [9] G. Coletti, et al. Effect of iron in silicon feedstock on p- and n-type multicrystalline silicon solar cells. *Journal of Applied Physics* 2008; **104**: 104913.
- [10] A. Bentzen, et al. Gettering of transition metal impurities during phosphorus emitter diffusion in multicrystalline silicon solar cell processing. *Journal of Applied Physics* 2006; **99**: 093509.
- [11] J. Schön et al. 2D modelling of the iron concentration from crystallization to final firing of mc silicon solar cells. *Proceedings of the 25th EUPVSEC*, Valencia, Spain, 2010.
- [12] J.Tan et al. Dissolution of metal precipitates in multicrystalline silicon during annealing and the protective effect of phosphorus emitters. *Applied Physics Letters* 2007; **91**: 043505.
- [13] D. Macdonald, L. J. Geerligs, and A. Azzizi. Iron detection in crystalline silicon by carrier lifetime measurements for arbitrary injection and doping. *Journal of Applied Physics* 2004, **95-3**: 1021–1028.
- [14] D.P. Fenning et al. Synchrotron-based microanalysis of iron distribution after thermal processing and predictive modeling of resulting solar cell efficiency. *Proceedings of the 35th IEEE PVSC*, Honolulu, USA, 2010, pp. 430-431.